Research Paper
Computational Methods for Differential Equations
http://cmde.tabrizu.ac.ir
Vol. 10, No. 3, 2022, pp. 580-594
DOI:10.22034/cmde.2021.41296.1794

Application of variation of parameter's method for hydrothermal analysis on MHD squeezing nanofluid flow in parallel plates

Ali Zabihi[1], Akinbowale T. Akinshilo[2], Hadi Rezazadeh[3], Reza Ansari[4], M. Gbeminiyi Sobamowo[5], and Cemil Tunç[6,∗]
[1]Department of Mechanical Engineering, Ahrar Institute of Technology and Higher Education, Rasht, Iran.
[2]Department of Mechanical Engineering, University of Lagos, Akoka- Yaba, Lagos, Nigeria.
[3]Faculty of Engineering Technology, Amol University of Special Modern Technologies, Amol, Iran.
[4]Department of Mechanical Engineering, University of Guilan, Rasht, Iran.
[5]Department of Mechanical Engineering,Yaba College of Technology, Yaba, Nigeria.
[6]Department of Mathematics, Faculty of Sciences, Van Yuzuncu Yil University, 65080-Campus, Van, Turkey.

Abstract

In this paper, the transport of flow and heat transfer through parallel plates arranged horizontally against each other is studied. The mechanics of fluid transport and heat transfer are formulated utilizing systems of the coupled higher-order numerical model. This governing transport model is investigated by applying the variation of the parameter's method. Result obtained from the analytical study is reported graphically. It is observed from the generated result that the velocity profile and thermal profile drop by increasing the squeeze parameter. The drop inflow is due to limitations in velocity as plates are close to each other. Also, thermal transfer due to flow pattern causes decreasing boundary layer thickness at the thermal layer, consequently drop in thermal profile. The analytical obtained result from this study is compared with the study in literature for simplified cases, this shows good agreement. The obtained results may therefore provide useful insight to practical applications including food processing, lubrication, and polymer processing industries amongst other relevant applications.

Keywords. Transport of flow and heat transfer; Coupled higher-order numerical model; Variation of parameter's method; Velocity profile and thermal profile; Squeeze parameter.

2010 Mathematics Subject Classification. 35Q35,76M30, 76W05, 80A20.

1. Introduction

Fluid flow through flow mediums have generated increasing interest in physical sciences and engineering, this is due to its wide range of applications in the modern day, but practical applications including lubrication, food processing, and polymer processing amongst other economically viable industries. As these applications are economic drivers, therefore it is of paramount importance to study the process applications and the controlling parameters involved in the study. Which improves the efficiency of the study. In the light of the above Choi [15] enhanced the thermal conductivity of fluid using nanoparticles. Viscoelastic nanofluid flow through a stretching sheet was studied by Madhu et al. [26]. The convective flow of a magnetohydrodynamic nanofluid in porous media under slip conditions was simulated by Uddin et al. [46]. Nanofluid flow through natural convecting differentially heated square cavity was investigated by Bendaraa et al. [13]. Ali and Makinde [11] modeled the variable viscosity effects on coquette fluid flowing unsteadily under convective cooling. Investigation of natural fluid flow under convective conditions was presented by Baskaya et al. [12] in the presence of a magnetic field applied constantly. Mixed convective nanofluid flow over a thin needle was studied by Nayak et al. [32] utilized a thin isothermal needle with nanomaterials of metallic and

Received: 16 August 2020 ; Accepted: 17 November 2021.
∗ Corresponding author. Email: cemtunc@yahoo.com.

metallic oxide nanomaterial. Thermal diffusion effect and viscous dissipation of micropolar non-Newtonian flow were presented by Abou-Zeid [1]. Pulsatile heat transfer and non-Newtonian fluid transport conveyed through a non-Darcy porous medium were analyzed by Eldade and Abou-Zeid[18]. Shortly after, Abou-Zeid [2] studied the coupled stress effect on peristaltic magnetohydrodynamic flow. Instability analysis of circular nanoelectromechanical plates into hydrostatic actuation was studied by Zabihi et al. [48]. Flow and thermal transfer of Carreu nanofluid considering internally generated heat transported over stretch sheet were presented by Sobamowo et al. [42]. The effect of thermal and fluid velocity was analyzed by Usman et al. [47] over-stretching permeable and incline cylinder. Nanofluid flow under bi-conventional conditions was studied by Uddin et al. [45] over a wedge under magnetic induction and multi-slip. Nanofluid transport and radiative heat transfer were presented by Hosseini et al. [25] subjected to chemical reaction and varying surface heat flux.

Since physical problems of this nature are described by higher-order differentials of ordinary coupled system equations. It ,therefore, becomes pertinent to analyze it utilizing numerical or analytical methods of solution. In the past, many analytical/numerical methods have been employed by researchers in providing solutions to physical problems of this nature. Methods include the perturbation method (PM), Homotopy analysis method (HAM), Optimal Homotopy asymptotic method (OHAM), residual weighted method (Galerkin, collocation, least squares method), variation iteration method (VIM), adomian decomposition method (ADM), and variation of parameter's method (VPM) [28, 29]. Analytical methods have been discovered to depend strongly on small perturbation parameter, which is usually non existent in practical science, round off errors, non-linearities, and other intricacies. However, the variation of parameter been a method of solution that can solve partial as well as ordinary coupled equations accurately, free from small perturbation parameter, having a highly successive iteration scheme with less computational procedural cost and time is adopted in this paper.

The flow of fluids under magnetic field effect has been proven over the years to be very pertinent to engineering applications including molten salt and metal pumps. As electromotive forces are generated due to applied magnetic field which velocity distribution. For some recent and interesting works, see, also, [8–10, 21, 37].

With respect to literature past, this paper aims to study the analysis of hydrothermal squeezing flow of nanofluid conveyed past parallel plates. These squeezing nanofluid flow phenomena and thermal transport are constantly subjected to magnetohydrodynamic field strength applied constantly, which is analyzed applying the VPM. The credibility of the results is validated by comparing the VPM with other methods in the literature. As a result, the effects of thermophoresis parameter, Brownian motion, magnetic field, suction/blowing parameter, and Squeezing parameter are discussed in detail.

2. Problem Description

In this section, the flow and thermal transport of nanofluid past parallel plates arranged horizontally against each other are presented. The plates having a distance of $h(t) = H(1-at)^{0.5}$ are squeezing under variable applied magnetic field $b(t) = B(1-at)^{0.5}$ perpendicular to plates as depicted in the model diagram Figure 1. The squeezing flow and its flow patterns are axisymmetric with considering left part of the channel, for simplicity sake. It is assumed fluid is incompressible, unsteady, fluid, and nanoparticles are at thermal equilibrium to each other, radiative and viscous dissipation is considered negligible due to constriction of flow part, non-chemically reactive, and non-slip flow. It should be carefully noted high moving fluid of large mass, effect of dissipation is constant. Thereupon, the governing equations of the fluid can be represented as [40]:

$$\overrightarrow{\nabla}.\overrightarrow{V} = 0, \tag{2.1}$$

$$\rho\left(\frac{\partial \overrightarrow{\nu}}{\partial t}\right) + \left(\overrightarrow{\nu}.\overrightarrow{\nabla}\right)\overrightarrow{\nu} = -\overrightarrow{\nabla}p + \mu\nabla^2\overrightarrow{\nu} + \sigma\left(\overrightarrow{J}\times\overrightarrow{B}\right), \tag{2.2}$$

$$(\rho c_p)\left(\frac{\partial T}{\partial t}\right) + \left(\overrightarrow{\nu}.\overrightarrow{\nabla}\right)T = K\nabla^2 T + \tau\left[D_B + \left(\overrightarrow{\nabla}T.\overrightarrow{\nabla}C\right) + \frac{D_T}{T_m}\left(\overrightarrow{\nabla}T.\overrightarrow{\nabla}T\right)\right], \tag{2.3}$$

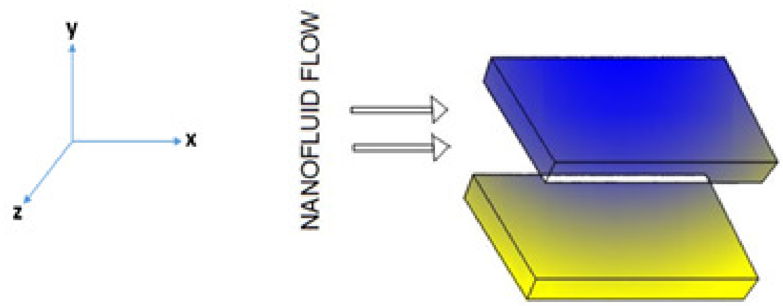

Figure 1. Schematic of the problem

$$(\rho c_p)\left(\frac{\partial C}{\partial t}\right)+\left(\overrightarrow{\nu}.\overrightarrow{\nabla}\right)C=D_B\nabla^2 C+\frac{D_T}{T_m}\nabla^2 T, \tag{2.4}$$

where $\overrightarrow{J}=\left(\overrightarrow{V}\times\overrightarrow{B}\right)$ in which $\overrightarrow{V}=(U,V,W)$ is the velocity-vector. Besides, $\rho, T, P, \mu, C_P, K,\ \alpha, C, D_B,\ T_m$, k and τ are density, temperature, -pressure, viscosity, heat-capacitance, thermal-conductivity of nanofluid, thermal diffusivity, nanoparticles concentration, Brownian motion coefficient, mean fluid temperature, thermal conductivity, and non-dimensional parameter correspondingly. Also, the Laplacian operator is indicated through $\overrightarrow{\nabla}$ and given by

$$\overrightarrow{\nabla}=\left(\frac{\partial}{\partial X},\frac{\partial}{\partial y},\frac{\partial}{\partial z}\right). \tag{2.5}$$

The boundary conditions are as follows:

$$z=h(t): u=0,\ w=\frac{dh}{dt},\ T=T_h,\ C=C_h,$$

$$z=0: u=0,\ w=-\frac{w_0}{\sqrt{1-at}},\ T=T_w,\ C=C_w, \tag{2.6}$$

where velocity components in the- z- and r- directions are-signified via v and u. With the velocity ${}^{dh}/_{dt}$, the upper disk can move towards or away from the motionless bottom disk at $Z=h(t)$. The whole diffusion mass flux for nanoparticles-is the last term in-the energy equation. The parameters of similarity-solution are as-follows:

$$u=\frac{ar}{2(1-at)}f'(\eta),\quad w=-\frac{aH}{\sqrt{1-at}}f(\eta),\quad \eta=\frac{z}{H\sqrt{1-at}}, \tag{2.7}$$

$$B(t)=\frac{B_0}{\sqrt{1-at}},\quad \theta=\frac{T-T_h}{T_{W-}T_h},\quad \phi=\frac{C-C_h}{C_{W-}C_h}.$$

Furthermore, $h(t)=H(1-at)^{1/2}$ and $B(t)=B_0(1-at)^{-1/2}$ signify the distance between two parallel plates and the variable-magnetic field. The '×','-' and '+' imply the magnetic field which is perpendicular to the plane, the negative and-positive-charges. Moreover, T_w and T_H indicate the temperature at the bottom and upper disks, C_w and C_H signify the concentration at the bottom and upper disks of nanoparticles. If $a<0$ then two plates are separated, and if $a>0$, then two plates are squeezed. The nonlinear equation is acquired by eliminating the pressure gradient from Eqs. (2.2), (2.3), then rewriting Eqs. (2.4), (2.5), [38]:

$$\begin{cases} f''''-S(\eta f'''+3f''-2ff''')-M^2f''=0,\\ \theta''+prS(2f\theta'-\eta\theta')+prNb\theta'\phi'+prNt\theta'^2=0,\\ \phi''+LeS(2f\phi'-\eta\phi')+\frac{Nt}{Nb}\theta''=0.\end{cases} \tag{2.8}$$

Besides, boundary conditions are described as follows:

$$f(0) = A, \;\; f'(0) = 0, \;\; \theta(0) = \phi(0) = 1,$$

$$f'(1) = \frac{1}{2}, \;\; f'(1) = 0, \;\; \theta(1) = \phi(1) = 0, \tag{2.9}$$

where S, M, Nb, Nt, Pr, Le evince the Squeeze number, the Hartmann number, the Brownian motion parameter, the Thermophoretic parameter, Prandtl number, and Lewis number which are defined as follows:

$$A = \frac{W_0}{aH}, \quad S = \frac{aH^2}{2\upsilon}, \quad M = \sqrt{\frac{\sigma B_0^2 H^2}{\upsilon}}, \quad \Pr = \frac{\upsilon}{\alpha}, \tag{2.10}$$
$$Nb = \frac{(\rho c)_p D_B (C_W - C_h)}{(\rho c)_f \upsilon}, \quad Nt = \frac{(\rho c)_p D_T (T_{w-} T_h)}{(\rho c)_f T_m \upsilon},$$

where A is the suction/blowing parameter, in which suction and blowing of fluid have occurred when $A > 0$, and $A < 0$ relatively. The intensity of magnetic field is represented as M, influence of momentum to thermal diffusivity is presented as Pr, concentration flow of nanoparticles are revealed as Nt, Nb, and Le, receding and coming together of plate is presented as S.

3. Solution Procedure

The technical procedures or procedural concept of the VPM for the analysis of coupled, nonlinear, and differential higher-order equation systems are

$$Lf(\eta) + Wf(\eta) + Nf(\eta) = Z, \tag{3.1}$$

where L is the highest order derivative and easily convertible, W is the linear operator remainder and less compared with L, $Z$is the system input or source term, and N is the nonlinear equation term. After decomposing Eq.(3.1) into linear and nonlinear terms L and N respectively, the VPM can be expressed as shown

$$f_{n+1}(\eta) = f_0(\eta) + \int_0^\eta \lambda(\eta s)(-wf_n(s) - Nf_n(s) - g(s)ds, \tag{3.2}$$

with as initial approximation given by

$$f_0(\eta) = \sum_{i=0}^{m} \frac{k_i f^i(0)}{i!}, \tag{3.3}$$

where m is the order of the given differential equation, k_i is an unknown-constant, $\lambda(\eta, s)$ is the multiplier which reduces the equation integration order. This is obtained upon the application of the Wronskian-technique [16]:

$$\lambda(\eta, s) = \sum_{i=0}^{m} \frac{(-1)^{i-1} s^{i-1} \eta^{m-1}}{(i-1)!(m-i)!} = \frac{(\eta - s)^{m-1}}{(m-1)!}. \tag{3.4}$$

4. Application of the VPM

The governing equations Eq. (2.8) are expressed by applying the standard procedural method of the variation of parameters expressed in Eq. (3.4). With respect to the above, the governing equations Eq. (2.8) can be expressed as

$$f_{n+1}(\eta) = k_1 + k_2 s + k_3 s^2 + k_4 s^3 - \int_0^\eta \left(\frac{\eta^3}{3!} - \frac{3\eta^2}{2!} + \frac{s^2 \eta}{2!} - \frac{s^3}{3!} \right) \times \left[\frac{d^4 f}{d\eta^4} - S\left(\eta \frac{d^3 f}{d\eta^3} + 3\frac{d^2 f}{d\eta^2} - 2f\frac{d^3 f}{d\eta^3} \right) - M\frac{d^2 f}{d\eta^2} \right] ds, \tag{4.1}$$

$$\theta_{n+1}(\eta) = k_1 + k_2 s - \int_0^\eta (\eta - s)\left[\frac{d^2\theta}{d\eta^2} + \Pr s\left(2f\frac{d\theta}{df} - \eta\frac{d\theta}{d\eta}\right) + \Pr Nb\frac{d\theta}{df}\frac{d\phi}{df} + \Pr Nt\left(\frac{d\theta}{df}\right)^2\right]ds, \tag{4.2}$$

$$\phi_{n+1}(\eta) = k_1 + k_2 s - \int_0^\eta (\eta - s)\left[\frac{d^2\phi}{d\eta^2} + LeS\left(2f\frac{d\phi}{df} - \eta\frac{d\phi}{df}\right) + \frac{Nt}{Nb}\frac{d^2\theta}{d\eta^2}\right]ds. \tag{4.3}$$

The constants k_1, k_2, k_3 and k_4 are constants of integration. They are obtained by taking-the highest-order in the linear term Eqs. (4.1)-(4.3). This is integrated to derive the final scheme-form. The iterative-scheme is obtained via implementing the boundary condition Eq. (2.9), With the first-order term shown as below

$$f_0 = A - \left(\eta^2(6A+1)\right)/2 + \left(\eta^3(12A+3)\right)/6, \tag{4.4}$$

$$\theta_0 = 1 - \eta, \tag{4.5}$$

$$\phi_0 = 1 - \eta. \tag{4.6}$$

Like the first-order term, the second-order and highest-order terms are expressed from the simplification of Eqs. (4.1)-(4.3) as below

$$\begin{aligned} f_1 = A &+ \left(\begin{array}{c} \eta^3(12A + S/40 - (4S\eta)/35 - 6AM^2/5 + 7S\eta^2/40 - S\eta^3/20 \\ -M^2/20 + 9AS/140 - 9AS\eta/35 + AS\eta^2/4 + 3AS\eta^3/10 + 3 \end{array}\right)/6 \\ &- \left(\begin{array}{c} \eta^2(6A + S/140 - 9S\eta/280 - AM^2/10 \\ +S\eta^2/20 - S\eta^3/40 + M^2/60 + 2AS/105 \\ -MAS\eta/140 + AS\eta^2/10 - AS\eta^3/60 + 1 \end{array}\right)/2 \\ &+\eta^5\left(S\eta^2/80 - AM^2/10 + S\eta^3/60 - M^2/40 + 3AS\eta^2/40 + AS\eta^3/15\right. \\ &\left.- \eta^4\left(2M^2 + S\eta^3(6A+1)\right)\right)/48 \\ &+ \left(S\eta^7(6A + 12\eta + 48A\eta + 1)/1680 - \left(S\eta^8(4A+1)\right)/840\right) \\ &- \left(S\eta^7\left(6A + 4\eta + 16A\eta + 1\right)\right)/240, \end{aligned} \tag{4.7}$$

$$\begin{aligned} \theta_1 =& (\Pr S(4A+1)\eta^6)/30 - (\Pr S(6A + \eta + 4A\eta + 1)\eta^5)/20 \\ &+ (\Pr S(\eta + 6A\eta - 1)\eta^4)/12 \\ &+ (\Pr S(2A + \eta)\eta^3))/6 + \Pr(Nb + Nt - 2AS\eta)\eta^2)/2 + ((\Pr S)/10 - (Nb\Pr)/2 \\ &- (Nt\Pr)/2 - (A\Pr S)/6 - (\Pr S\eta)/5 + (7A\Pr S\eta)/10 - 1)\eta + 1, \end{aligned} \tag{4.8}$$

$$\begin{aligned} \phi_1 =& LeS(4A+1)\eta^6/30 - LeS(6A + \eta^5 A + 1)\eta^5/20 + LeS(\eta + 6A\eta - 1)\eta^4/12 \\ &+ LeS(2A + \eta)\eta^3/6 - ALeS\eta^3 + LeS/10 - ALeS/6 \\ &- LeS\eta/5 + 7ALeS\eta/10 - 1)\eta + 1, \end{aligned} \tag{4.9}$$

and the highest-order terms of the solution of Eq. (4.1)-(4.3) are presented as follows

$$\begin{aligned} f_2 =& A - 3A\eta^2 + 2A\eta^3 - S\eta^2/280 + S\eta^3/240 + 5\eta^7/1680 - 8\eta^8/840 - \eta^2/2 + \eta^3/2 \\ &- M^2\eta^2/120 - M^2\eta^3/120 + M^2\eta^4/24 - 13M^4\eta^2/50400 - M^2\eta^5/40 \\ &- M^4\eta^3/16800 + ..., \end{aligned} \tag{4.10}$$

$$\begin{aligned}\theta_2 =&A^2\mathrm{Pr}^2S^2\eta^{10}/4 - A^2\mathrm{Pr}^2S^2\eta^{11}/18 - 2A^2\mathrm{Pr}^2S^2\eta^9/7 - A^2\mathrm{Pr}^2S^2\eta^8/3 \\ &+ 47A^2\mathrm{Pr}^2S^2\eta^4/10 - 313A^2\mathrm{Pr}^2S^2\eta^3/1575 + 2A^2\mathrm{Pr}^2S^2\eta^{11}/25 \\ &- 31A^2\mathrm{Pr}^2S^2\eta^7/150 + ...,\end{aligned} \tag{4.11}$$

$$\begin{aligned}\phi_2 =&\eta^6 LeS/15 + LeS/3600 - Le^2S^2/300 + 43ALe^2S^2/900 + 7LeS^2\eta^2/31 \\ &+ Le^2S^2\eta/900 - LeS^2\eta^3/1800 + LeS\eta^4/720 + 4ALeS/15 + A^2Le^2S^2/45 \\ &- Le^2S^2\eta^3/36 + ALeS^2/1400 - LeM^2S/1800 - 2LeS^2\eta/1575 \\ &+ Nt\,\mathrm{Pr}\,S/30Nb + ...\end{aligned} \tag{4.12}$$

As observed in the analysis for velocity, thermal, and concentration profiles in Eqs. (4.4)- (4.12). The final expression of the velocity, thermal, and concentration profile can be represented as

$$f(\eta) = f_0(\eta) + f_1(\eta) + f_2(\eta), \tag{4.13}$$

$$\theta(\eta) = \theta_0(\eta) + \theta_1(\eta) + \theta_2(\eta), \tag{4.14}$$

$$\phi(\eta) = \phi_0(\eta) + \phi_1(\eta) + \phi_2(\eta). \tag{4.15}$$

Besides, important characteristics of mass and heat transfer such as skin friction, nusselt number and the sherwood number are expressed as follows

$$\begin{aligned}&cfr = f''(1), \\ &Nur = -\theta(1), \\ &Shr = -\phi(1).\end{aligned} \tag{4.16}$$

5. Results and Discussions

In this section, the effect of hydrothermal analysis of nanofluid flowing through the parallel plates is examined under the effect of magnetic field, which is reported graphically for varying parametric quantities. The analysis is investigated using the variation of parameters method which is validated for the simplistic case with Hosseinzadeh et al. [33] expressed in Table (1) for fluid concentration profile at parameters $A = M = S = Le = Nb = Nt = 1$, $Pr = 2.2$. Also, the effect of varying parameters for thermal scale for slowing receding plates is shown in Table (2). As observed from the scale, thermal distribution rises at the lower plate, then towards the midplate ($\eta = 0.4$) the temperature decreases slightly. As seen in Table (3), the scale for thermal distribution is shown, this reveals as plates come together temperature decreases steadily from the lower plate to the upper plate. This is due to thermal loss relate to heat exchange caused by plate motion which is analyzed at constant parameters of $A = 1, M = 0.5, Le = 1, Nb = Nt = 0.2$, and $Pr = 1.2$.

In Figure 2, the velocity profile versus η is depicted to show the impact of the Magnetic parameter. As seen the variation of velocity profile is increased through raising the Magnetic parameter, this is due to the effect of increasing Lorentz force effect on the boundary, therefore increasing thickness of momentum layer thickness. Also, the effect of Magnetic parameter can be neglected by raising η.

The velocity profile versus η is presented to verify the impact of A in Figure 3. It can be inferred that the velocity profile is increased by raising the suction parameter $A > 0$, however it is decreased via increasing the blowing parameter $A < 0$. Suction parameter increase causes a surge in velocity due to turbulence in flow.

In Figures 4 and 5, the impact of squeeze parameter on velocity and thermal profile against η are shown. It can be concluded that the velocity profile and thermal profile are dropped by increasing the squeeze parameter. Drop in flow is due to limitations in velocity as plates are close to each other. Also, thermal transfer due to flow pattern causes decreasing boundary layer thickness at the thermal layer, consequently drop in thermal profile.

In Figure 6, the concentration profile versus is plotted. It is transparent that as plates recede ($s < 0$) concentration decreases due to fluid boundary layer thickness reduces. On the other hand, when plates move together ($s > 0$) boundary layer improves due to the conservation of mass flow as velocity gradient increases. This is due to diminishing thickness of concentration layer.

In Figures 7 and 8, effects of thermophoresis parameter on thermal profile and concentration profile versus are depicted. One can find that from Figure 7, mass transfer and heat convection induce high fluid temperature particle, so particle dispersion increases hence heat transfer rate increases relatively. However, in Figure 8, slower fluid particle motion increases concentration boundary layer, thereupon the concentration profile is decreased by raising the thermophoresis parameter.

In Figures 9 and 10, the effects of Brownian parameter on thermal profile and concentration profile are depicted. According to these schemes, the thermal profile is increased by increasing Brownian parameter which can be physically explained due to increase in thermal boundary thickness at the lower plate, howbeit the concentration profile is decreased via increasing Brownian parameter. This is as a result of increasing rate of diffusion of concentration species.

To show the impacts of Lewis number the concentration profile versus is presented in Figure 11. Based on this graph, one can find that the concentration profile is decreased by increasing the Lewis number. As concentration of nanoparticles in the base fluid is increased by raising the Lewis number, hence decrease in concentration of boundary layer is obtained by high nanoparticle concentration. In Figures 12 and 13, impact of Brownian and thermophoresis parameters on nusselt number versus squeeze parameter are depicted. One can find that by increasing Brownian and thermophoresis parameters, nusselt number increases relatively.

Effect of squeeze parameter on skin friction versus suction/blowing and Magnetic parameters are shown in Figures 14 and 15. It is seen that skin friction is increased via increasing Brownian and thermophoresis parameters.

In Figure 16, effect of squeeze parameter on Sherwood number versus Lewis number is presented. It can be inferred that Sherwood number decreases by increasing squeeze parameter.

Table 1. Comparison of values of η for dimensionless concentration profile ($A = M = S = Le = Nb = Nt = 1, Pr = 6.2$).

η	$\phi(\eta)$				
	HPM[38]	CM[38]	FEM[38]	VPM	Error
0	1.000000000	1.000000000	1.000000000	1.0000	0.000000000
0.1	0.779370558	0.9000934056	0.9112683052	0.9012	0.0100683052
0.2	0.6012650162	0.7989509826	0.8108534964	0.7932	0.0176534964
0.3	0.4559056726	0.6970283829	0.7064057452	0.6934	0.0130057452
0.4	0.3359299240	0.5947812584	.6016217396	0.5923	0.0093217396
0.5	0.2360877164	0.4926652610	0.4980783825	0.4972	0.0008783825
0.6	0.1530318820	0.3911360429	0.3962207368	0.3916	0.0046207368
0.7	0.08537940058	0.2906492357	0.2959127913	0.2954	0.0005127913
0.8	0.03409554226	0.1916605515	0.196753453	0.1965	0.0002534530
0.9	0.003119131100	0.09462558233	0.0982635139	0.0973	0.0009635139
1.0	0.00000000000	0.0000000000	0.0000000000	0.0000	0.0000000000

TABLE 2. Comparison of values of η for dimensionless temperature profile ($A = 1, M = 0.5, Le = 1, Nb = Nt = 0.2, Pr = 1.2, S = -2$).

η	$(\theta)\eta$ Numerical	VPM	Error
0.0	1.0000	1.0000	0.0000
0.1	1.0571	1.0571	0.0000
0.2	1.0664	1.0664	0.0000
0.3	1.0315	1.0315	0.0000
0.4	0.9572	0.9572	0.0000
0.5	0.8488	0.8488	0.0000
0.6	0.7122	0.7122	0.0000
0.7	0.5534	0.5534	0.0000
0.8	0.3783	0.3783	0.0000
0.9	0.1922	0.1922	0.0000
1.0	0.0000	0.0000	0.0000

TABLE 3. Comparison of values of η for dimensionless temperature profile ($A = 1, M = 0.5, Le = 1, Nb = Nt = 0.2, Pr = 1.2, S = 2$).

η	$(\theta)\eta$ Numerical	VPM	Error
0.0	1.0000	1.0000	0.0000
0.1	0.7762	0.7762	0.0000
0.2	0.5943	0.5943	0.0000
0.3	0.4494	0.4494	.0000
0.4	0.3362	0.3362	0.0000
0.5	0.2488	0.2488	0.0000
0.6	0.1812	0.1812	0.0000
0.7	0.1275	0.1275	0.0000
0.8	0.0824	0.0824	0.0000
0.9	0.0411	0.0411	0.0000
1.0	0.0000	0.0000	0.0000

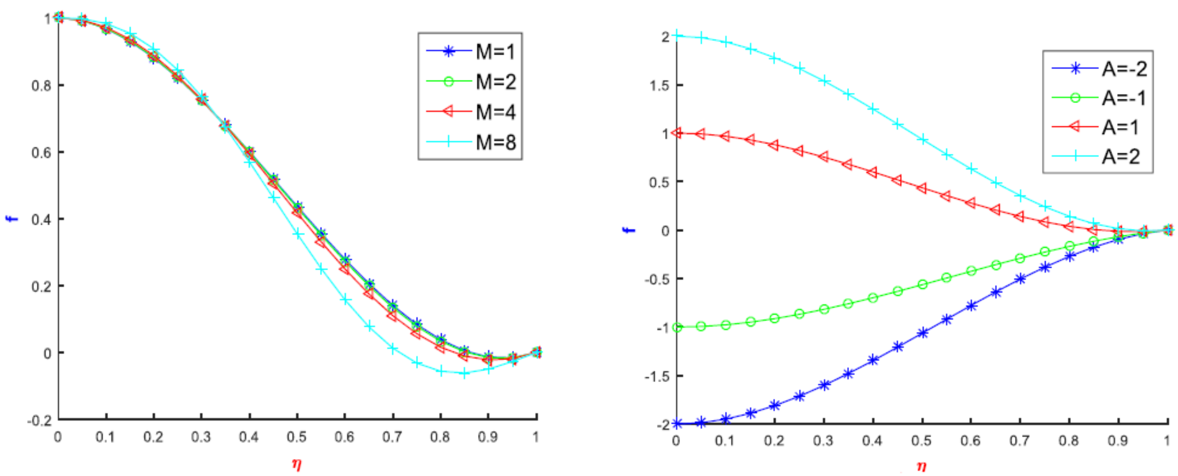

(a) (b)

FIGURE 2. (a) Effect of Magnetic parameter on velocity profile against η,(b) Effect of suction/blowing parameter on velocity profile versus η

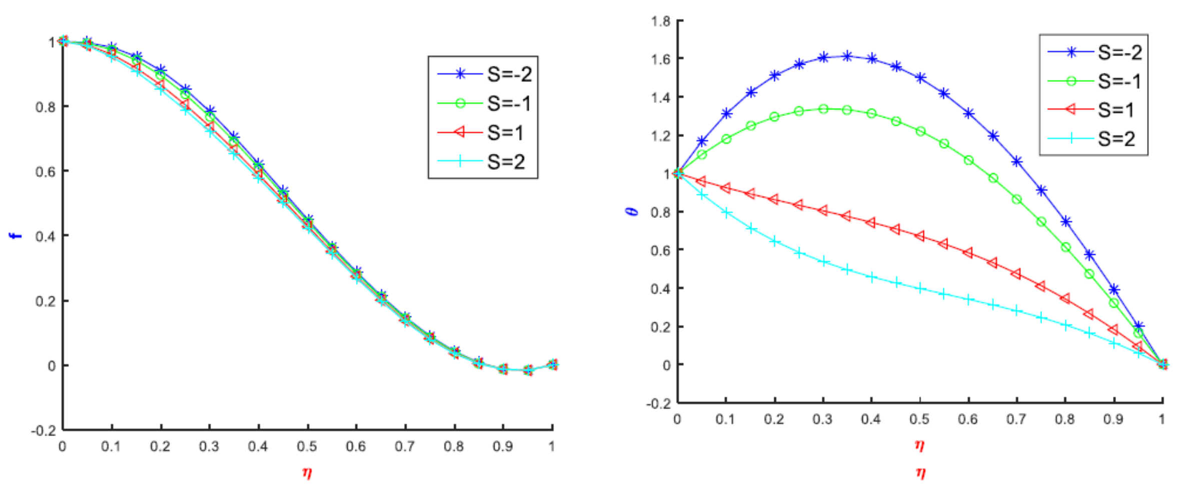

(a) (b)

FIGURE 3. (a) Effect of squeeze parameter on velocity profile against η, (b) Impact of squeeze parameter on thermal profile versus η

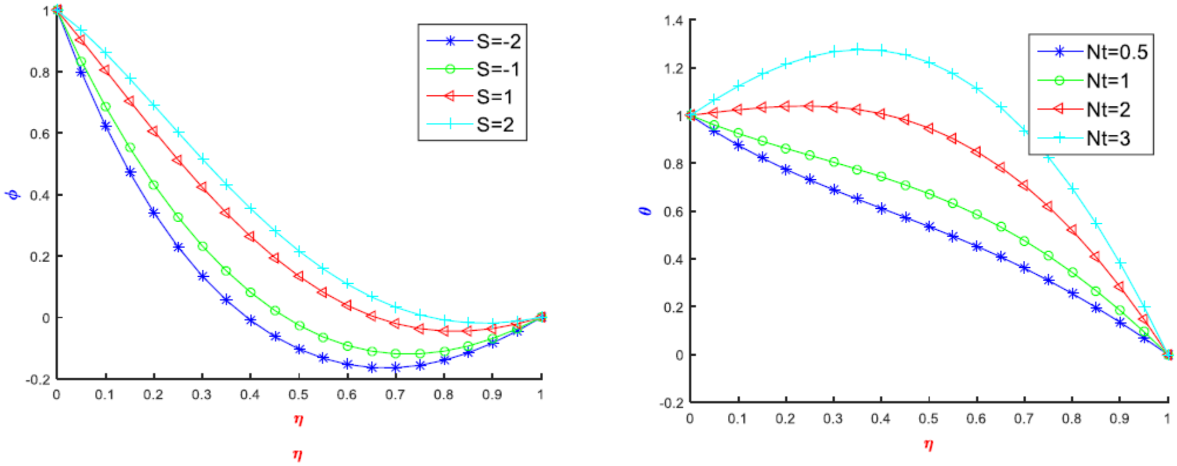

(a) (b)

FIGURE 4. (a) Variation of squeeze parameter on concentration profile against η, (b) Effect of thermophoresis parameter on thermal profile against η

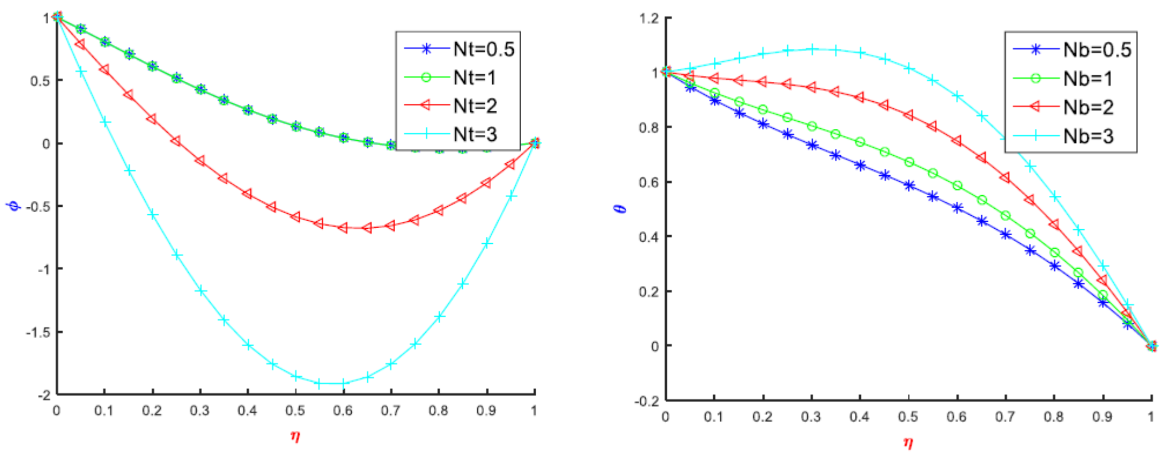

(a) (b)

FIGURE 5. (a)Impact of thermophoresis parameter on concentration profile versus η, (b) Variation of Brownian parameter on thermal profile against η.

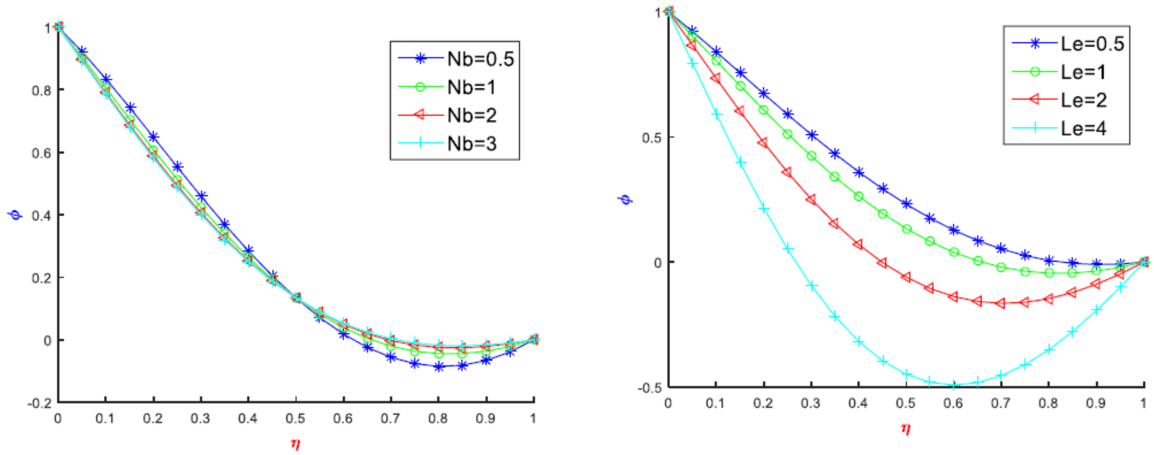

(a) (b)

FIGURE 6. (a) Impact of Brownian parameter on concentration profile versus η, (b) Effect of Lewis number on concentration profile against η.

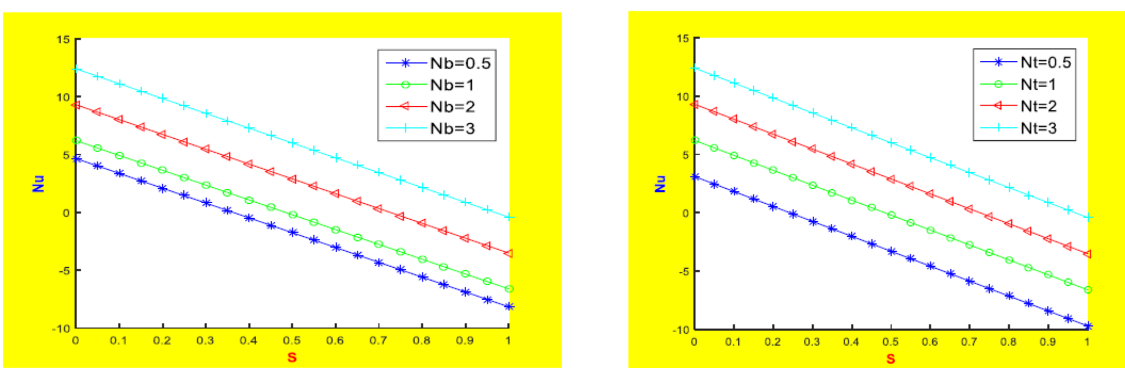

(a) (b)

FIGURE 7. (a) Impact of Brownian parameter on nusselt number versus squeeze parameter, (b) Variation of thermophoresis parameter on nusselt number against squeeze parameter.

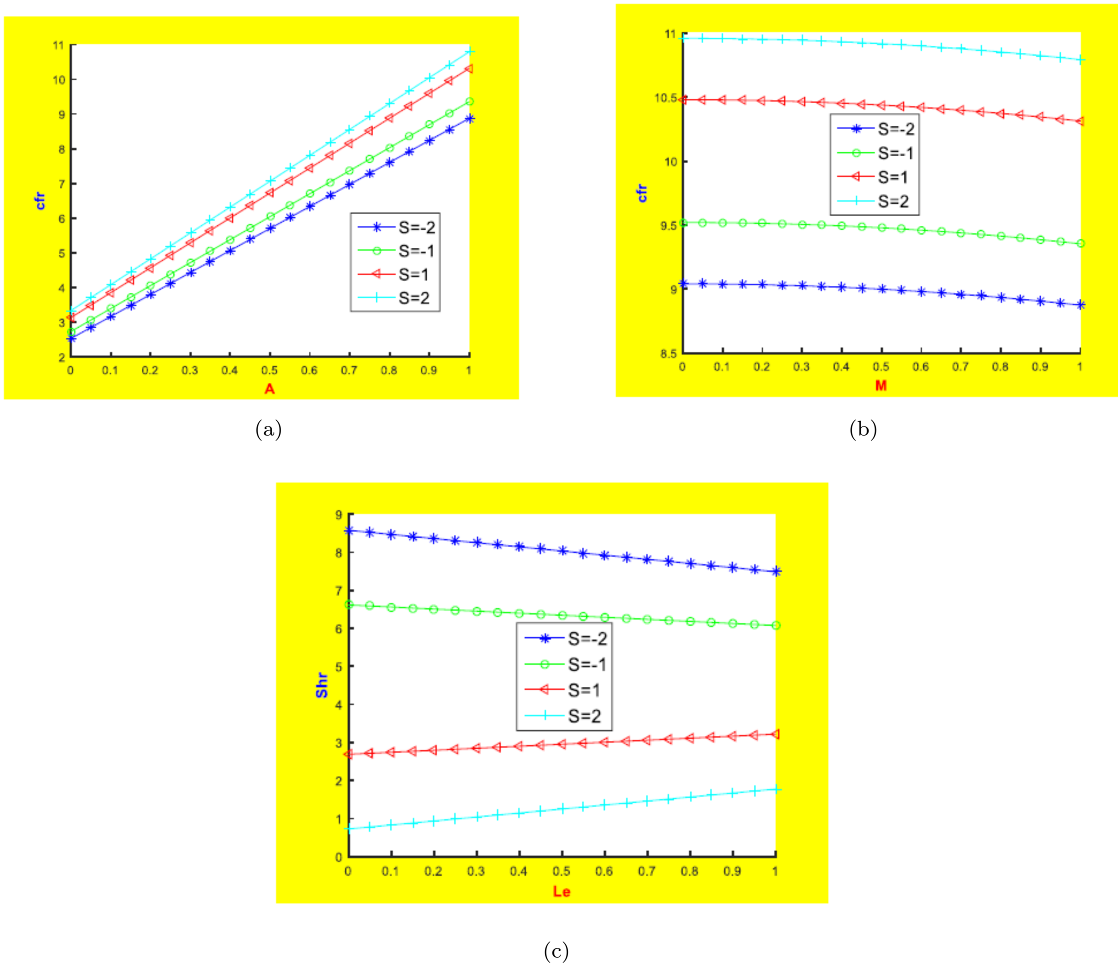

FIGURE 8. (a) Effect of squeeze parameter on skin friction versus suction/blowing parameter, (b) Impact of squeeze parameter on skin friction against Magnetic parameter, (c) Effect of squeeze parameter on Sherwood number versus Lewis number.

6. Conclusion

This study considers the squeezing flow through horizontally arranged parallel plates. The transport and heat transfer mechanics are described as adopting coupled system of ordinary differential, coupled system of equations. This is analyzed with the help of VPM as an analytical methodology. It is observed from generated result that the velocity profile and thermal profile drops by increasing the squeeze parameter. Drop in flow is due to limitations in velocity as plates are close to each other. Also, thermal transfer due to flow pattern causes decreasing boundary layer thickness at the thermal layer, consequently drop in thermal profile. Analysis of result obtained is verified for accuracy with literature obtained for simplistic case which proves excellent agreement. Results obtained may therefore provide useful insight to practical application including food processing, lubrication, and polymer processing industries amongst other relevant applications.

References

[1] M. Abou-Zeid, *Effects of thermal-diffusion and viscous dissipation on peristaltic flow of micropolar non-Newtonian nanofluid: Application of homotopy perturbation method*, Results in Physics, *6* (2016), 481–495.

[2] M. Y. Abou-Zeid, *Homotopy perturbation method for couple stresses effect on MHD peristaltic flow of a non-newtoniannanofluid*, Microsystem Technologies, *24* (2018), 4839–4846.

[3] S. Ahmad, N. M. Arifin, R. Nazar, and I. Pop, *Mixed convection boundary layer flow along vertical thin needles: assisting and opposing flows*, International Communications in Heat and Mass Transfer, *3592* (2008), 157–162.

[4] R. Ahmad, M. Mustafa, and S. Hina, *Boungiomo's model for fluid flow around a moving needle in a flowing nanofluid: a numerical study*, Chinese Journal of Physics, *55* (2017), 1264–1274.

[5] A. T. Akinshilo, *Flow and heat transfer of nanofluid with injection through an expanding or contracting porous channel under magnetic force field*, Engineering Science and Technology, an International Journal, *21* (2018), 486–494.

[6] A. T Akinshilo and J. O. Olofinkua, *Variation of Parameters method for thermal analysis of straight convective radiative fins with temperature dependent thermal conductivity*, Journal of Computational Mechanics, *49* (2018), 125–132.
DOI:10.22059/JCAMECH.2018.250910.236.

[7] A. T. Akinshilo, J. O. Olofinkua, and O. Olaye, *Flow and Heat Transfer Analysis of Sodium Alginate Conveying Copper Nanoparticles between Two Parallel Plates*, Journal of Applied and Computational Mechanics, *3* (2017), 25–266.

[8] A. T. Akinshilo, A. G. Davodi, H. Rezazadeh, G. Sobamowo, and C. Tunç, *Heat transfer and flow of MHD micropolarnanofluid through the porous walls*, magnetic fields and thermal radiation, Palest. J. Math., *11*(2) (2022) , 604–616.

[9] M. N. Alam and C. Tunc, *An analytical method for solving exact solutions of the nonlinear Bogoyavlenskii equation and the nonlinear diffusive predator–prey system*, Alexandria Engineering Journal, *11*(1) (2016), 152–161.

[10] M. N. Alam and C. Tunç, *The new solitary wave structures for the (2+1)-dimensional time-fractional Schrodinger equation and the space-time nonlinear conformable fractional Bogoyavlenskii equations*, Alexandria Engineering Journal, *59* (2020), 2221–2232.

[11] A. O. Ali and O. D. Makinde, *Modelling the effects of variable viscosity on unsteady couette flow of nanofluids with convective colling*, Journal of Applied Fluid Mechanics, *8* (2015), 793–802.

[12] E. Baskaya, M. Fidanoglu, G. Komurgoz, and I. Ozkol, *Investigation of MHD natural convection flow exposed to constant magnetic field via generalized differential quadrature method*, Engineering Systems Design and Analysis, (2014).
DOI :10.1115/ESDA 2014–20177.

[13] A. Bendaraa, M. M. Charafi, and A. Hasnaoui, *Numerical study of natural convection in a differentially heated square cavity filled with nanofluid in the presence of fins attached to walls in different locations*, Physics of Fluids, *31* (2019), 052003.

[14] M. Biglarian, M. R. Gorji, O. Pourmehran, and G. Domairry, *H2O based different nanofluids with unsteady condition and an external magnetic field on permeable channel heat transfer*, International Journal of Hydrogen Energy, *42* (2017), 22005–2201.

[15] S. U. S. Choi and J. A. Eastman, *Enhancing thermal conductivity of fluids with nanoparticles*, Developments and applications of non-Newtonian flows, *66* (1995), 99–105.

[16] A. S. Dogonchi, M. Alizadeh, and D. D. Ganji, *Investigation of MHD Go-water nanofluid flow and heat transfer in a porous channel in the presence of thermal radiation effect*, Advance Powder Technology.
DOI: 10.1016/j.apt.2017.04.022.

[17] G. Domairry and M. Hatami, *Squeezing Cu-water nanofluid flow analysis between parallel plates by DTM-Pade Method*, Journal of Molecular Liquids *188* (2014), 155–161.

[18] N. T. Eldade and M. Y. Abou-Zeid, *Homotopy perturbation method for MHD pulsatile non-Newtonian nanofluid flow with heat transfer through a non-Darcy porous medium*, Journal of Egyptian Mathematical Society, *25* (2017), 375-381,
DOI: 10.1016/j.joems.2017.05.003.

[19] M. Fakour, D. D. Ganji, A. Khalili, and A. Bakhshi, *Heat transfer in nanofluvd MHD flow in a channel with permeable wall*, Heat Transfer Research *48* (2017), 221–238.

[20] M. Fakour, A. Rahbari, K. Erfan, and D. D. Ganji, *Nanofluid thin film flow and heat transfer over an unsteady stretching elastic sheet by LSM*, Journal of Mechanical Science and Technology, *32* (2018), 177–183.

[21] M. Fayz-Al-Asad, M. N. Alam, C. Tunç, and M. M. A. Sarker, *Heat Transport Exploration of Free Convection Flow inside Enclosure Having Vertical Wavy Walls*, J. Appl. Comput. Mech., *7*(2) (2021), 520-527.

[22] S. S. Ghadikolahi, Kh. Hosseinzadeh, and D. D. Ganji, *Analysis of unsteady MHD Eyring-Powell squeezing flow in stretching channel with considering thermal radiation and Joule heating effect using AGM*, Case Studies in Thermal Engineering, *10* (2017), 579–594.
DOI: 10.1016/j.csite.2017.11.004.

[23] Kh. Hosseinzadeh, M. Alizadeeh, and D. D. Ganji, *Hydrothermal analysis on MHD squeezing nanofluid flow in parallel plates by analytical method*, International Journal of Mechanical and Material Engineering, *4* (2018), 1–12.

[24] Kh. Hosseinzadeh, M. Alizadeh, and D. D. Ganji, *Hydrothermal analysis on MHD squeezing nanofluid flow in parallel plates by analytical method*, International Journal of Mechanical and Materials Engineering, *143* (2020), 39–52.

[25] E. Hosseini, Gh. BaridLoghmani, M. Heydari, and M. M. Rashidi, *A numerical simulation of MHD flow and Radiation heat transfer of nanofluid through a porous medium with variable surface heat flux and chemical reaction*, Journal of Mathematical Extension, *13* (2019), 31–67.

[26] M. Madhu and N. Kishan, *Finite element analysis of MHD viscoelastic nanofluid flow over a stretching sheet with radiation*, Procedia Engineering, *127* (2015), 432–439.

[27] P. Mohan Khrishna, R. Prakash Sharma, and N. Sandeep, *Boundary layer analysis of persistent moving horizontal needle in Blasius and Sakiadis magnetohydrodynamic radiative nanofluid flow*, Nuclear Engineering Technology, *49* (2017), 1654–1659.

[28] T. J. Moore and M. R. Jones, *Solving nonlinear heat transfer problems using variation of parameters*, International Journal of Thermal Sciences, *93* (2015), 29–35.

[29] S. Mosayebidorcheh, M. Rahimi-Gorji, D. D. Ganji, and T. Moayebidorcheh, *Transient thermal behavior of radial fins of rectangular, triangular and hyperbolic profiles with temperature-dependent properties using DTM-FDM*, Journal of Central South University, *24*(3) (2017), 675–682.

[30] M. Mustafa, T. Hayat and S. Obadiat, *On heat and mass transfer in an unsteady squeezing flow between parallel plates*, Mechanica, *47* (2012), 1581–1589.

[31] M. K. Nayak, F. Mabood, and O. D. Makinde, *Heat transfer and buoyancy-driven convective MHD flow of nanofluids impinging over a thin needle moving in a parallel stream influenced by Prandtl number*, Heat Transfer—Asian Research (2019), 1–18.

[32] M. K. Nayak, A. Wakif, I. L. Animasaun, and M. Saidi Hassani Alaoui, *Numerical differential quadrature examination of steady mixed convection nanofluid flows over and isothermal thin needle conveying metallic and metallic*

oxide nanomaterials: A comparative investigation*, Arabian Journal for Science and Engineering, (2020), DOI: 10.1007/s13369–020–04420.

[33] O. Pourmehran, M. M. Sarafraz, M. Rahimi-Gorji, and D. D. Ganji, *Rheological behaviour of various metal-based nano-fluids between rotating discs: a new insight*, Journal of the Taiwan Institute of Chemical Engineers (2018), Article ID:644800.

[34] A. Rahbari, M. Fakour, A. Hamzehnezhad, A. Akbari, M. Vakilabadi, and D. D. Ganji, *Heat transfer and fluid flow with nanoparticles through porous vessels in a magnetvc field: A quasi one dimensional analytvcal approach*, Mathematical Biosciences, *283* (2017), 38–47.

[35] M. Rahimi-Gorji, O. Pourmehran, M. Hatami, and D. D. Ganji, *Statistical optimization of microchannel heat sink (MCHS) geometry cooled by different nanofluids using RSM analysis*, The European Physical Journal Plus, *130* (2016), 15022-15030.

[36] J. V. Ramana Reddy, V. Sugunamma, and N. Sandeep, *Thermophoresis and Brownian motion effects on unsteady MHD nanofluid flow over a slandering surface with slip effects*, Alexandria Engineering Journal, (2017), DOI: 10.1016/j.aej.2017.02.014.

[37] H. Rezazadeh, J. Sab'u, A. Zabihi, R. Ansari, and C. Tunç, *Implementation of solition solutions for nonlinear Schrödinger equation with variable coefficients*, Nonlinear Stud., *29*(2) (2022), 457-476.

[38] S. N. A. Salleh, N. Bachok, N. Md. Arifin, F. Md. Ali, and I. Pop, *Stability analysis of mixed convection flow towards moving a thin needle in nanofluid*, Applied Science, *8* (2018), 842.

[39] M. Sheikholeslami and M. M. Bhatti, *Forced convection of nanofluid in presence of constant magnetic field considering shape effects of nanoparticles*, International Journal of Heat and Mass Transfer, *111* (2017), 1039–1049.

[40] W. Sikander, N. Ahmed, U. Khan, and S. T. Mohyud-Din, *Coupling of optimal variation of parameters method with Adomian'spolynominals for nonlinear equations representing fluid flow in different geometrics*, Neural Comput and Applic, *30* (2018), 3431–3444.

[41] W. Sikandar, U. Khan, N. Ahmed, and S. T. Mohyud-Din, *Variation of parameters method with an auxiliary parameter for initial value problems*, Ain Shams Engineering Journal, *9* (2018), 1959–1963. DOI: 10.1016/j.asej.2016.09.014.

[42] M. G. Sobamowo, L. O. Jayesimi, and M. A. Waheed, *Chebyshev specteral collocation method for flow and heat transfer in magnetohydrodynamic dissipative carreunanofluid over a streteching sheet with internal heat generation*, AUT Journal of Mechanical Engineering, *3* (2019), 3–14.

[43] C. Sulochana, G. P. Ashwinkumar, and N. Sandeep, *Joule heating effect on a continuously moving thin needle in MHD Sakiadis flow with thermophoresis and Brownian moment*, The European Physical Journal Plus, (2017), DOI: 10.1140/epjp/i2017-11633-3.

[44] R. Trimibitas, T. Grosan, and I. Pop, *Mixed convective boundary layer flow along vertical thin needle in nanofluids* , International Journal of Numerical Methods for Heat and Fluid Flow, *24* (2014), 579–594.

[45] M. J. Uddin, M. N. Kabir, O. A. Beg, and Y. Alginahi, *Chebyshev collocation computation of magneto-bioconvectionnanofluid flow over a wedge with multiple slips and magnetic induction*, Journal of Nanomaterials Nanoengineering and Nanosystems, *232* (2018), 109–122.

[46] M. J. Uddin, P. Rana, O. Anwar Beg, and A. I. Md. Ismail, *Finite element simulation of magnetohydrodynamic convective nanofluid slip flow in porous media with nonlinear radiation*, Alexandria Engineering Journal, *55* (2016), 1305–1319.

[47] M. Usman, F. A. Soomro, R. U. Haq, W. Wang, and O. Defterli, *Thermal and velocity slip effects on Casson-nanofluid flow over an inclined permeable stretching cylinder via collocation method*, International Journal of Heat and Mass Transfer, *122* (2018), 1255–1263.

[48] A. Zabihi, J. Torabi, and R. Ansari, *Effects of geometric nonlinearity on the pull-in instability of circular microplates based on modified strain gradient theory*, Physica Scripta, *95* (2020), 115204.